

Statistical hypothesis test for maritime pine forest SAR images classification based on the geodesic distance

Ioana Ilea, Lionel Bombrun, Christian Germain, Isabelle Champion, Romulus Terebes, Monica Borda

▶ **To cite this version:**

Ioana Ilea, Lionel Bombrun, Christian Germain, Isabelle Champion, Romulus Terebes, et al.. Statistical hypothesis test for maritime pine forest SAR images classification based on the geodesic distance. IEEE International Geoscience and Remote Sensing Symposium 2015, 2015, Milan, Italy. pp.3215-3218. hal-01188075

HAL Id: hal-01188075
https://hal.science/hal-01188075

Submitted on 28 Aug 2015

HAL is a multi-disciplinary open access archive for the deposit and dissemination of scientific research documents, whether they are published or not. The documents may come from teaching and research institutions in France or abroad, or from public or private research centers.

L'archive ouverte pluridisciplinaire **HAL**, est destinée au dépôt et à la diffusion de documents scientifiques de niveau recherche, publiés ou non, émanant des établissements d'enseignement et de recherche français ou étrangers, des laboratoires publics ou privés.

STATISTICAL HYPOTHESIS TEST FOR MARITIME PINE FOREST SAR IMAGES CLASSIFICATION BASED ON THE GEODESIC DISTANCE

Ioana Ilea[1,2]*, Lionel Bombrun*[1]*, Christian Germain*[1]*, Isabelle Champion*[3]*, Romulus Terebes*[2]*, Monica Borda*[2]

[1]: Université de Bordeaux, Laboratoire IMS, Groupe Signal et Image. {*ioana.ilea, lionel.bombrun, christian.germain* }*@ims-bordeaux.fr*

[2]: Technical University of Cluj-Napoca. {*romulus.terebes, monica.borda* }*@com.utcluj.ro*

[3]: INRA Bordeaux, UMR 1391 ISPA. *champion@bordeaux.inra.fr*

ABSTRACT

This paper introduces a new statistical hypothesis test for image classification based on the geodesic distance. We present how it can be used for the classification of texture image. The proposed method is then employed for the classification of Polarimetric Synthetic Aperture Radar images of maritime pine forests on both simulated data with the PolSARproSim software and real data acquired during the ONERA RAMSES campaign in 2004.

***Index Terms*—** Hypothesis test, SAR, geodesic distance, classification.

1. INTRODUCTION

Texture-oriented analyzes on optical images have proven their efficiency for the classification of maritime pine forest. Various approaches have been considered in the literature such as gray-level co-occurrence matrices (GLCM) [1, 2, 3] and more recently wavelet based approaches [4, 5, 6]. In this paper, we investigate how these methods can be extended to SAR and Polarimetric SAR (PolSAR) data [7].

Multiscale approaches have been found to be effective for many image processing applications. In a classification context, the image is decomposed into a set of wavelet subbands, each of them being modeled by a parametric model. During the last decades, many univariate and multivariate parametric models have been proposed including elliptical models [8, 9] and copula based approaches [10, 11]. Next, for each subband, the estimated parameter vector composes the signature of the image. Once the feature vectors are computed for each texture image, a distance (or at least a divergence) is calculated in order to measure the degree of similarity between two images. The similarity measure which computes the proximity between two images should be intrinsic to the parametric model. A well-known choice is the Kullback-Leibler (KL) divergence. Recently, some authors have proposed to consider the geodesic distance which is the shortest path in the parametric manifold. This latter has shown superior retrieval rate compared to the KL divergence for texture image classification [9]. Inspired from previous works on the KL divergence and on the family of (h, ϕ) divergences [12, 13], we introduce a new statistical hypothesis test based on the geodesic distance which is the main objective of the paper. A second contribution concerns the use of a SAR scenes simulator [14] to study the influence of the acquisition parameters (incidence angle, spatial resolution) on classification accuracy.

The paper is structured as follows. Section 2 introduces the proposed statistical hypothesis test based on the geodesic distance. Section 3 presents an application for the classification of pine forests based on Polarimetric Synthetic Aperture Radar (PolSAR) images. Classification results are then discussed in Section 4 on both synthetic and real datasets. Conclusions and future works are finally reported in Section 5.

2. STATISTICAL HYPOTHESIS TEST FOR SAR IMAGE CLASSIFICATION

In this paper, we propose to set up a statistical hypothesis test. Let $\chi_1 = (\mathbf{x}_1^1, \ldots, \mathbf{x}_m^1)$ and $\chi_2 = (\mathbf{x}_1^2, \ldots, \mathbf{x}_n^2)$ be two sets of m and n independent and identically distributed random variables (vectors) $\mathbf{x}$ according to the parametric models $p(\mathbf{x}|\theta_1)$ and $p(\mathbf{x}|\theta_2)$. Let $\hat{\theta}_1$ and $\hat{\theta}_2$ be the maximum likelihood estimators computed on these sets. In a classification problem, the aim is to determine if χ_1 and χ_2 are issued from the same parametric model. Let's consider the following hypothesis test [13]

$$\begin{cases} H_0 : \theta_1 = \theta_2, \\ H_1 : \theta_1 \neq \theta_2. \end{cases} \tag{1}$$

When $\theta_1 = \theta_2$, we can prove that the statistic $S_{GD}(\widehat{\theta_1}, \widehat{\theta_2}) = \dfrac{mn}{m+n} GD^2(\widehat{\theta_1}, \widehat{\theta_2})$ is asymptotically chi-square distributed with M degrees of freedom for sufficiently large value of m and n. The degree of freedom M is equal to the dimension of the parameter space ($M = d(d+1)/2$). In the following, we propose an application to the zero-mean multivariate Gaussian distribution (MGD). In such case, the geodesic distance is given by $GD(\hat{\mathbf{M}}_1, \hat{\mathbf{M}}_2) = \left[\frac{1}{2}\sum_i (\ln \lambda_i)^2\right]^{\frac{1}{2}}$, where $\hat{\mathbf{M}}_1$ and $\hat{\mathbf{M}}_2$ are the maximum likelihood estimates of two MGDs covariance matrices and λ_i, $i = 1 \ldots d$ are the eigenvalues of $\hat{\mathbf{M}}_2^{-1}\hat{\mathbf{M}}_1$.

3. APPLICATION TO MARITIME PINE FOREST CLASSIFICATION

The dataset used for this work contains both simulated and real L-band SAR images. First, the simulated dataset is used to determine the best airborne configuration for maritime pine classification according to the stand age. In other words, is it better to have a single high resolution SAR image or a low resolution PolSAR image with two or three channels? Second, real SAR images are used to validate the results.

3.1. Database

3.1.1. Simulated L-band SAR images

The simulated dataset is created by using the PolSARproSim software. This software provides fully polarized simulated SAR images of forest displaying properties consistent with real SAR imagery [14]. Images are obtained by specifying various acquisition parameters such as the platform altitude, the incidence angle, the frequency, the azimuth and slant range resolutions, and some forest stand properties, including the stand area and density, the tree species and their mean height.

For our study, pine tree forests of 5, 6, 12, 15, 21, 25 and 32 years old are simulated. The platform altitude is set to 3580 meters, corresponding to an airborne system, while the frequency is fixed at 1.3 GHz (L-band). In order to find the best airborne configuration, two experiments are considered. In the first case, the incidence angle is chosen to be $45°$ and the influence of the spatial resolution on classification performance is evaluated. Five datasets are simulated at a resolution of respectively 0.5, 1, 2, 3 and 5 meters. In the second case, the image resolution is fixed to 0.5 meters and several incidence angles are tested: $25°$, $35°$, $45°$ and $55°$.

In both cases, the stand density (D) and the mean tree height ($\bar{H}$) are set according to the desired stand age, as mentioned in Table 1.

Age	5	6	12	15	21	25	32
$\bar{H}$	5.5	6.5	11.6	13.7	17.3	19.2	21.9
D	1200	1200	800	800	400	400	300

Table 1: Maritime pine stand density D (stems/ha) and mean tree height $\bar{H}$ (meters) as a function of stand age (years).

The values for the stand density are chosen to be equal to those given by the *Centre Régional de la Propriété Forestière Aquitaine*, France for the maritime pine, while the mean tree height $\bar{H}$ is obtained by using the Maugé theoretical model [15] given by $\bar{H} = H_{max}(1 - 0.96^a)$, where $H_{max} = 30$ meters is the maximum height and a is the stand age.

By using these numerical values, a database of 350 images is created for each experiment and structured in 4 classes, according to the stand age: $\mathbf{1^{st}}$ **class:** less than 10 years (Fig. 1(a)); $\mathbf{2^{nd}}$ **class:** between 10 and 20 years (Fig. 1(b)); $\mathbf{3^{rd}}$ **class:** between 20 and 30 years (Fig. 1(c)); $\mathbf{4^{th}}$ **class:** over 30 years (Fig. 1(d)).

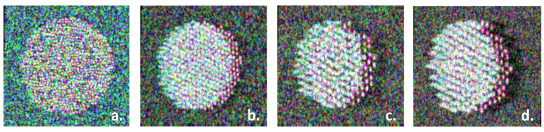


Fig. 1: Examples of L-band pine forest images of: (a) 5, (b) 15, (c) 21 and (d) 32 years old simulated with PolSARproSim software for an incidence angle of $45°$ and a resolution of 1 meter.

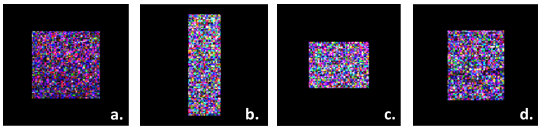


Fig. 2: The real L-band SAR image and examples of pine forest stands of: 5 (a), 15 (b), 21 (c) and 32 (d) years old.

3.1.2. Real L-band SAR image

The real L-band SAR data displayed in Fig. 2 consists in one fully polarimetric image (1 meter resolution) acquired on the Nezer maritime pine forest in France, during an ONERA RAMSES campaign in 2004. From this image, 62 forest stands between 5 and 48 years old are identified and grouped in 4 classes, as it was done for the simulated images.

In the next section, we present several strategies for modeling SAR images and hence obtaining the corresponding feature vectors.

3.2. Methodology

3.2.1. GLCM

The GLCMs are computed on the real-valued HV polarization image transformed in dB and quantified with 32 gray levels. The number of quantization levels is chosen by taking into consideration the image size. In a Cartesian coordinate system, the GLCMs are functions of two parameters: the distance d between neighboring pixels and the direction α. For our study, d varies between 1 and 15, and $\alpha = \{0°, 45°, 90°, 135°\}$. The Haralick [1] textural descriptors *homogeneity*, *entropy*, and *correlation* along with the *GLCM mean* are extracted and averaged in the four directions to reduce the sensibility to the stand's orientation [6]. Further on, this method is denoted by *GLCM HV*.

3.2.2. MGD model for a single polarization image

The real-valued HH polarization image transformed in dB is decomposed by using a Daubechies 4 (db4) wavelet trans-

form, with 2 levels and 3 orientations. For each subband, a spatial dependence with a 3×3 neighborhood is considered and modeled by the MGD. The parameter of this distribution is estimated by the Sample Covariance Matrix (SCM). In the following, this algorithm is denoted by *MGD HH + WT + S*.

3.2.3. MGD model for a three polarization image

The HH, HV and VV polarization images are merged into a 3-dimensional array, with each pixel being a complex number. Three different algorithms are developed based on:

- *the polarimetric dependence* (denoted *MGD Polar*): the complex 3-dimensional array is modeled by the MGD and a 3×3 covariance matrix is estimated with the SCM algorithm.
- *the polarimetric dependence and the wavelet decomposition* (denoted *MGD Polar + TW*): the complex 3-dimensional array is filtered using the db4 wavelet transform with 2 levels and 3 orientations. Each subband is modeled by the MGD and the 3×3 covariance matrix is estimated with the SCM algorithm.
- *the polarimetric and spatial dependence, along with the wavelet decomposition* (denoted *MGD Polar + TW + S*): the complex 3-dimensional array is decomposed using a db4 wavelet transform having 2 levels and 3 orientations. For each subband, a spatial dependence given by a 3×3 neighborhood is modeled by the MGD and a 27×27 covariance matrix is estimated with the SCM algorithm.

4. RESULTS

In the context of a supervised classification, the database is randomly divided into a training and a testing set by a cross-validation procedure. The partitioning algorithm is repeated 100 times and for each iteration half of the database is used for training, while the other half is used for testing. Once the feature vector extracted for all images, a similarity measure between testing and training images is computed by using the Mahalanobis distance for the GLCM algorithm and the statistic S_{GD} defined in Section 2 for the others. All the previously described algorithms are tested and the retrieval performance is evaluated by means of the overall accuracy computed for a k Nearest Neighbor classifier (k-NN), with k set to 5. In the following, the classification performances obtained on both simulated and real SAR images are presented.

4.1. Simulated L-band SAR images

As mentioned in Section 3.1.1, two types of experiments are performed on simulated data. First, the influence of the image resolution is tested. For this experiment the incidence angle is fixed to $45°$ and the image resolution varies from 0.5m to 5m. Fig. 3 draws the influence of distance d to find the best distance between neighboring pixels. It can be seen that distances between 1 and 5 pixels give the best results. Fig. 4 shows a comparison between the GLCM algorithm and the statistical based approaches with the geodesic distance, knowing that each time the polarization with the best performance is retained. As observed in Fig. 4, for simulated data it is better to have one very high resolution polarization channel ($99 \pm 1\%$ for MGD HH + WT + S at 0.5 meters) than a low resolution fully polarimetric SAR image ($85 \pm 4.5\%$ for MGD Polar at 5 meters). For this example, a significant gain of about 14 points is observed.

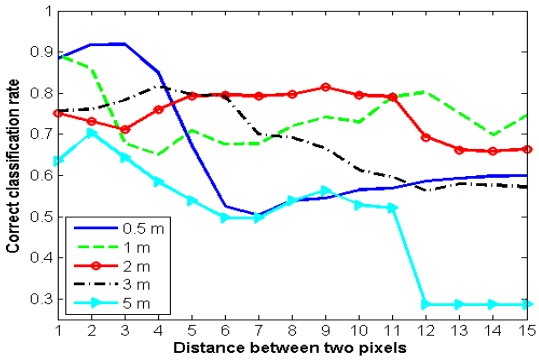


Fig. 3: Influence of distance d in GLCM on classification accuracy for different spatial resolution (HV channel).

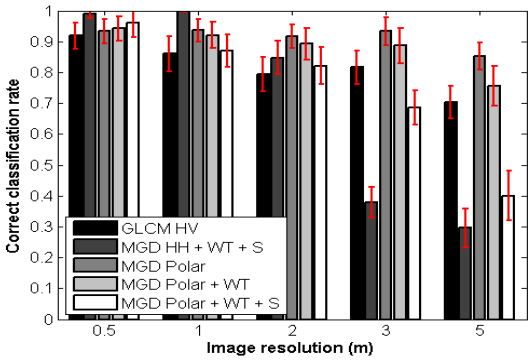


Fig. 4: Influence of the spatial resolution on classification accuracy for simulated L-band SAR images with incidence angles of $45°$.

Second, the influence of the incidence angle is analyzed. For this experiment, the image resolution is fixed to 0.5m and several incidence angles are considered. Like in the previous case, tests are performed to find the appropriate distance d for the GLCM algorithm. The best classification rates are retained and compared in Fig. 5 with those given by the statistical based methods. As it can be seen, the GLCM HV is influenced by the incidence angle, while some small changes can be spotted for the other methods.

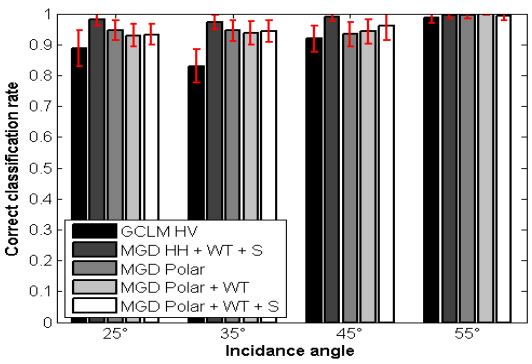


Fig. 5: Influence of the incidence angle on classification accuracy for simulated L-band SAR images having a resolution of 0.5 meter.

4.2. Real L-band SAR images

Even though PolSARproSim provides a high level of realism, significant differences can be observed between simulated (Fig. 1) and real data (Fig. 2). Those differences are the results of various phenomena, such as forest management practices (thinning operations, plantation density) and natural hazards (storm damages), yielding to some within-class diversity. Hence, as displayed in Table 2, classification results on real SAR images are lower to those shown in Section 4.1 on synthetic dataset. Similar to the case of simulated images with a resolution of 3 and 5m, the best results are given for GLCM HV ($86.6 \pm 5.6\%$) and MGD Polar ($84.0 \pm 4.4\%$) methods.

Classification method	Overall accuracy
GLCM HV	$\mathbf{86.6 \pm 5.6}$
MGD HH + WT + S	59.0 ± 5.4
MGD Polar	$\mathbf{84.0 \pm 4.4}$
MGD Polar + WT	81.8 ± 4.0
MGD Polar + WT + S	63.5 ± 4.9

Table 2: Comparison between the classification algorithms for real L-band SAR images.

5. CONCLUSION

In this paper, we have introduced a statistical hypothesis test based on the geodesic distance. Various experiments have been conducted on both simulated and real SAR data for the classification of maritime pine forest images. Experiments on simulated dataset have shown that it is better to have one very high resolution polarization channel than a low resolution fully polarimetric SAR image. Due to the presence of intra-class diversity, those conclusions are slightly modified on real SAR data.

Further works will include the generalization of the proposed hypothesis test to robust estimators such as the family of M-estimators [16].

6. REFERENCES

[1] R. M. Haralick, K. Shanmugam, and I. Dinstein, "Textural Features for Image Classification," *IEEE Trans. on Syst., Man and Cyber.*, vol. SMC-3, no. 6, pp. 610–621, Nov. 1973.

[2] F. Kayitakire, C. Hamel, and P. Defourny, "Retrieving forest structure variables based on image texture analysis and IKONOS-2 imagery," *Rem. Sens. of Env.*, vol. 102, no. 3, pp. 390–401, 2006.

[3] I. Champion, P. Dubois-Fernandez, D. Guyon, and M. Cottrel, "Radar image texture as a function of forest stand age," *International Journal of Remote Sensing*, vol. 29, no. 6, pp. 1795–1800, 2008.

[4] M.N. Do and M. Vetterli, "Wavelet-Based Texture Retrieval Using Generalized Gaussian Density and Kullback-Leibler Distance," *IEEE Trans. on Im. Process.*, vol. 11, pp. 146–158, 2002.

[5] O. Regniers, L. Bombrun, D. Guyon, J.-C. Samalens, C. Tinel, G. Grenier, and C. Germain, "Wavelet based texture modeling for the classification of very high resolution maritime pine forest images," in *IEEE IGARSS*, July 2014, pp. 2027–2030.

[6] O. Regniers, L. Bombrun, D. Guyon, J.-C. Samalens, and C. Germain, "Wavelet-based texture features for the classification of age classes in a maritime pine forest," *IEEE Geosc. and Rem. Sens. Lett.*, vol. 12, no. 3, pp. 621–625, March 2015.

[7] I. Champion, C. Germain, J. P. Da Costa, A. Alborini, and P. Dubois-Fernandez, "Retrieval of forest stand age from sar image texture for varying distance and orientation values of the gray level co-occurrence matrix," *IEEE Geosc. and Rem. Sens. Lett.*, vol. 11, no. 1, pp. 5–9, 2014.

[8] L. Bombrun, Y. Berthoumieu, N.-E. Lasmar, and G. Verdoolaege, "Mutlivariate texture retrieval using the geodesic distance between elliptically distributed random variables," in *IEEE ICIP*, 2011, pp. 3637–3640.

[9] G. Verdoolaege and P. Scheunders, "On the geometry of multivariate generalized Gaussian models," *Journal of Math. Imag.and Vis.*, vol. 43, no. 3, pp. 180–193, 2012.

[10] R. Kwitt and A. Uhl, "Lightweight probabilistic texture retrieval," *IEEE Trans. on Im. Process.*, vol. 19, no. 1, pp. 241–253, 2010.

[11] Y. Stitou, N.-E. Lasmar, and Y. Berthoumieu, "Copulas based multivariate gamma modeling for texture classification," in *IEEE ICASSP*, 2009, pp. 1045–1048.

[12] M. Salicru, D. Morales, M.L. Menendez, and L. Pardo, "On the applications of divergence type measures in testing statistical hypotheses," *Journal of Multivariate Analysis*, vol. 51, no. 2, pp. 372 – 391, 1994.

[13] A.D.C. Nascimento, R.J. Cintra, and A.C. Frery, "Hypothesis testing in speckled data with stochastic distances," *IEEE Trans. on Geosc. and Rem. Sens.*, vol. 48, pp. 373–385, 2010.

[14] M.L. Williams, "PolSARproSim: A Coherent, Polarimetric SAR Simulation of Forests for PolSARPro. Design Document ans Algorithm Specification (u1.0) ," 2006.

[15] J.P. Maugé, *Le pin maritime premier résineux de France*, Centre de Productivité et d'Action Forestière d'Aquitaine, Institut pour le Développement Forestier, Paris, 1987.

[16] I. Ilea, L. Bombrun, C. Germain, R. Terebes, and M. Borda, "Statistical hypothesis test for robust classification on the space of covariance matrices," in *IEEE ICIP*, 2015.